

## RESEARCH ARTICLE

## Cancer stem cell subpopulations in primary colon adenocarcinoma

Matthew J. Munro<sup>1,2</sup>, Susrutha K. Wickremesekera<sup>1,3</sup>, Lifeng Peng<sup>2</sup>, Reginald W. Marsh<sup>1,4</sup>, Tinte Itinteang<sup>1</sup>, Swee T. Tan<sup>1,5\*</sup>

**1** Gillies McIndoe Research Institute, Newtown, Newtown, Wellington, New Zealand, **2** School of Biological Sciences and Centre for Biodiscovery, Victoria University of Wellington, Kelburn, Wellington, New Zealand, **3** Upper Gastrointestinal, Hepatobiliary & Pancreatic Section, Department of General Surgery, Wellington Regional Hospital, Private Bag 7902, Wellington, New Zealand, **4** University of Auckland, Grafton, Auckland, New Zealand, **5** Wellington Regional Plastic, Maxillofacial & Burns Unit, Hutt Hospital, Lower Hutt, New Zealand

\* [swee.tan@gmri.org.nz](mailto:swee.tan@gmri.org.nz)

## OPEN ACCESS

**Citation:** Munro MJ, Wickremesekera SK, Peng L, Marsh RW, Itinteang T, Tan ST (2019) Cancer stem cell subpopulations in primary colon adenocarcinoma. PLoS ONE 14(9): e0221963. <https://doi.org/10.1371/journal.pone.0221963>

**Editor:** Sujit Kumar Bhutia, National Institute of technology Rourkela, INDIA

**Received:** March 22, 2019

**Accepted:** August 19, 2019

**Published:** September 6, 2019

**Copyright:** © 2019 Munro et al. This is an open access article distributed under the terms of the [Creative Commons Attribution License](https://creativecommons.org/licenses/by/4.0/), which permits unrestricted use, distribution, and reproduction in any medium, provided the original author and source are credited.

**Data Availability Statement:** All relevant data are within the manuscript and its Supporting Information files.

**Funding:** MM was supported by a scholarship from the New Zealand Community Trust, 75841. The funder had no role in study design, data collection and analysis, decision to publish, or preparation of the manuscript.

**Competing interests:** The authors declare that the research was conducted in the absence of any commercial or financial relationships that could be construed as a potential conflict of interest. TI and

## Abstract

## Aims

The cancer stem cell concept proposes that tumor growth and recurrence is driven by a small population of cancer stem cells (CSCs). In this study we investigated the expression of induced-pluripotent stem cell (iPSC) markers and their localization in primary low-grade adenocarcinoma (LGCA) and high-grade adenocarcinoma (HGCA) and their patient-matched normal colon samples.

## Materials and methods

Transcription and translation of iPSC markers OCT4, SOX2, NANOG, KLF4 and c-MYC were investigated using immunohistochemical (IHC) staining, RT-qPCR and *in-situ* hybridization (ISH).

## Results

All five iPSC markers were detected at the transcriptional and translational levels. Protein abundance was found to be correlated with tumor grade. Based on their protein expression within the tumors, two sub-populations of cells were identified: a NANOG<sup>+</sup>/OCT4<sup>-</sup> epithelial subpopulation and an OCT4<sup>+</sup>/NANOG<sup>-</sup> stromal subpopulation. All cases were accurately graded based on four pieces of iPSC marker-related data.

## Conclusions

This study suggests the presence of two putative sub-populations of CSCs: a NANOG<sup>+</sup>/OCT4<sup>-</sup> epithelial subpopulation and an OCT4<sup>+</sup>/NANOG<sup>-</sup> stromal subpopulation. Normal colon, LGCA and HGCA could be accurately distinguished from one another using iPSC

STT are inventors of the provisional patents Cancer Diagnosis and Therapy (PCT/NZ2015/050108) and Cancer Therapeutic (PCT/NZ2018/050006), and provisional patent application Novel Pharmaceutical Compositions for Cancer Therapy (US/62/711709).

marker expression. Once validated, novel combinations of iPSC markers may provide diagnostic and prognostic value to help guide patient management.

## Introduction

The cancer stem cell (CSC) concept hypothesizes that tumor growth is driven by CSCs, a small subpopulation of cancer cells with stem cell characteristics [1–4]. CSCs produce identical daughter pluripotent cells, as well as progenitor cells which are more committed and sit on a hierarchy between CSCs and terminally differentiated cancer cells [5–7]. Cells within this hierarchy can be identified by their expression of different combinations of markers [6, 8]. Tang [5] postulates that progenitor cells are responsible for uncontrolled growth.

Takahashi and Yamanaka [9] first used octamer-binding transcription factor 4 (*OCT4*, *POU5F1*), sex-determining region Y-box 2 (*SOX2*), Krüppel-like factor 4 (*KLF4*) and *c-MYC* to produce induced-pluripotent stem cells (iPSCs). The Thomson laboratory produced iPSCs from human fibroblasts using *OCT4*, *SOX2*, *NANOG* and *LIN28* [10].

*OCT4* is a transcription factor involved in stem cell maintenance, and has been observed in normal colon stem cells [11]. Studies have shown *OCT4* expression in colorectal cancer (CRC), often in the cytoplasm of epithelial cells [11–13]. The *OCT4B* isoform is unable to act as a transcription factor and is often localized to the cytoplasm, while the *OCT4B1* spliced variant is over-expressed in high-grade CRC [14].

*SOX2* maintains pluripotency of ESCs and neural progenitor cells and is critical for early embryogenesis [11, 15]. It is involved in regulating *OCT4* transcription by binding to its promoter region [16–18]. Studies have localized *SOX2* to the cytoplasm and nuclei of both normal and cancerous crypt epithelial cells [19]. *SOX2* expression is associated with lymph node infiltration and metastasis in CRC [20].

*NANOG* transcription is controlled by the *OCT4/SOX2* transcription factor complex [16, 21]. *NANOG* has been detected in colon cancer and dysplastic polyps, often exhibiting strong nuclear staining in a subpopulation of epithelial cells within the crypts [11, 22].

*c-MYC* has been well-studied for its role as a proto-oncogene and is often over-expressed in cancer [9]. Duplication of the *c-MYC* gene is associated with a worse prognosis in CRC [23]. Therapy-naïve CRC cells with high *c-MYC* expression progress more quickly, and CRC metastases exhibit greater *c-MYC* expression than the primary tumor [24].

*KLF4* is associated with colon sphere-forming cells and involvement in cell cycle, pluripotency and self-renewal [16, 25]. *KLF4* is a marker of differentiation down the goblet cell epithelial lineage from intestinal stem cells [26]. In CRC, *KLF4* levels decrease with increasing histological grade, with poorly-differentiated (high-grade) tumors expressing less *KLF4* than well-differentiated (low-grade) tumors [27].

Primary colon adenocarcinoma (CA), the most common type of CRC, is categorized as low-grade (well- and moderately-differentiated tumors with greater than 50% crypt and gland composition) or high-grade (poorly-differentiated tumors with densely-packed tumor cells) [28]. Although CSCs have been previously studied in CRC, the putative subpopulations of CSCs are yet to be characterized. We hypothesized that CA contains subpopulations of CSCs which can be identified by their expression patterns of iPSC-related markers. In this study, we investigated the level of iPSC marker transcription and translation, and their distribution within the epithelium and stroma, to determine the difference between low-grade CA (LGCA) and high-grade CA (HGCA) and their patient-matched normal colon (NC), using

3,3-diaminobenzidine (DAB) and immunofluorescence (IF) immunohistochemical (IHC) staining, RT-qPCR, and *in-situ* hybridization (ISH).

## Materials and methods

### Tissue samples

Snap-frozen and formalin-fixed paraffin-embedded (FFPE) tissue samples of LGCA from ten patients and HGCA from eight patients, with patient-matched normal colon (NC) tissue samples from 17 of the 18 patients, were provided by the Gillies McIndoe Research Institute Tissue Bank for this study, which was approved by the Central Health and Disability Ethics Committee (Ref. 15/CEN/106).

### DAB IHC staining

DAB IHC staining was performed on the entire cohort. 4  $\mu$ m-thick FFPE sections of NC, LGCA and HGCA tissue samples were stained for iPSC markers OCT4, SOX2, NANOG, KLF4 and c-MYC. Positive human control tissues included in each run to validate the staining were seminoma for OCT4 and NANOG, normal skin for SOX2, normal breast tissue for KLF4 and prostatic tissue for c-MYC. Each IHC staining procedure also included a matched isotype antibody as a negative control. Protocols were performed as previously described [29].

Staining was carried out on the Leica BOND™ RX Auto-stainer using primary antibodies for OCT4 (1:30; cat#MRQ-10, Cell Marque, Rocklin, CA, USA), SOX2 (1:200; cat#ab97959, Abcam, Cambridge, MA, USA), NANOG (1:200; cat#EP225, Cell Marque), KLF4 (1:200; cat#NBP2-24749SS, Novus Biologicals LLC, Littleton, CO, USA) and c-MYC (1:1000; cat#ab32, Abcam).

### IF IHC staining

Protein localization was performed on three LGCA and three HGCA and their patient-matched normal colon samples by dual IF IHC staining, carried out on the Leica BOND™ RX Auto-stainer. Secondary antibodies used were Vectafluor Excel goat anti-mouse 488 (ready-to-use; cat#DK2488, Vector Laboratories, Burlingame, CA, USA) and Alexa Fluor donkey anti-rabbit 594 (1:500; cat#ab150076, Life Technologies, Carlsbad, CA, USA). All stained slides were mounted as previously described [29]. Negative controls were performed using matched isotype controls for both mouse (ready-to-use; cat#IR750, Dako, Copenhagen, Denmark) and rabbit (ready-to-use; cat#IR600, Dako).

### ISH

ISH staining was performed on 4  $\mu$ m-thick FFPE sections of six LGCA and six HGCA tissue samples and their patient-matched NC tissue samples. This was carried out on the Leica BOND™ RX Auto-stainer using probes for OCT4 (NM\_002701), SOX2 (NM\_003106), NANOG (NM\_024865), KLF4 (NM\_004235) and c-MYC (NM\_002467), using the ViewRNA eZ Detection Kit to detect the presence of mRNA (Affymetrix, Santa Clara, CA, USA). Positive controls were human seminoma for OCT4, NANOG and KLF4, normal skin for SOX2, and normal colon tissue for c-MYC. To determine specificity of the probes, negative controls were run using a probe for *Bacillus* (NM\_L38424).

### Image capture and analysis

DAB IHC and ISH images were captured using an Olympus BX53 light microscope fitted with an Olympus SC100 digital camera and CellSens 2.0 software (Olympus, Tokyo, Japan). Images

were used for manual cell counting using ImageJ software (National Institutes of Health, Bethesda, MD, USA). Six images were captured per stained slide. When capturing images, areas with muscle and blood vessels were avoided. All positively and negatively stained cells within these images were counted and identified as either epithelial (crypt) or stromal cells. Cells were counted as positive if they had any level of staining (weak, moderate or strong) in the nucleus and/or cytoplasm. IF IHC-stained slides were visualized and imaged using an Olympus FV1200 biological confocal laser-scanning microscope (Olympus) and processed using CellSens 2.0 software (Olympus).

### RNA extraction

RNA was extracted from the same cohorts of six LGCA and six HGCA tissue samples and their patient-matched NC tissues, using a QIAcube (Qiagen) as previously described [30].

### RT-qPCR

RT-qPCR reactions were run on the Rotor-Gene Q (Qiagen), as previously described [30] using Taqman primers (Thermo Fisher) for OCT4 (Hs00999632\_g1; 77kb), SOX2 (Hs01053049\_s1; 91kb), NANOG (Hs04399610\_g1; 101kb), KLF4 (Hs00358836\_m1; 110kb) and c-MYC (Hs00153408\_m1; 107kb).

### Statistical analysis

Statistical analysis was carried out using SPSS V22. Protein expression of iPSC markers in the stroma and the crypt were compared using a *t*-test for both normal and tumor samples. Statistical significance was defined as a  $p < 0.05$ .

The differences between LGCA and HGCA tissue samples were calculated using Analysis of Variance (ANOVA). A discriminant function analysis was also performed using the four sets of data which had the highest correlation for either LGCA or HGCA tumors. This produced a canonical correlation value and Wilkes Lambda variance value, representing the level of confidence for which these four pieces of data taken from any given specimen is able to be used to predict the grade of the tumor. mRNA levels were compared between normal stroma and tumor stroma, and between normal epithelium and tumor epithelium, using a *t*-test to determine statistical significance.

## Results

### DAB IHC staining

EPCAM was used to distinguish between epithelial cells and stromal cells (S1 Fig). It was found that EPCAM expression was restricted to epithelial cells in all NC, LGCA and HGCA tissues.

OCT4 (Fig 1A–1C, brown) was detected in the nucleus of 2.5% of NC epithelial cells, likely to be the normal intestinal stem cells (A). However, it was found in the cytoplasm of 25% of stromal cells in LGCA (B) and 30% of stromal cells in HGCA (C) with little or no presence in the epithelium (0.7%). SOX2 (Fig 1D–1F, brown) was expressed in the cytoplasm of epithelial and stromal cells in NC, LGCA and HGCA tissue samples. Overall, NC (D) samples stained more strongly than LGCA (E) and HGCA (F) tissue samples. SOX2 was abundant in the nuclei of NC epithelium. NANOG (Fig 1G–1I, brown) was not detected in NC (G) but was present in HGCA (75% of cases, weak-to-moderate; H) and LGCA (40% of cases, weak; I) tissue samples. c-MYC (Fig 1J–1L, brown) was observed in the nuclei and cytoplasm of NC (J), LGCA (K) and HGCA (L) epithelium. KLF4 (Fig 1M–1O, brown) showed perinuclear expression in NC

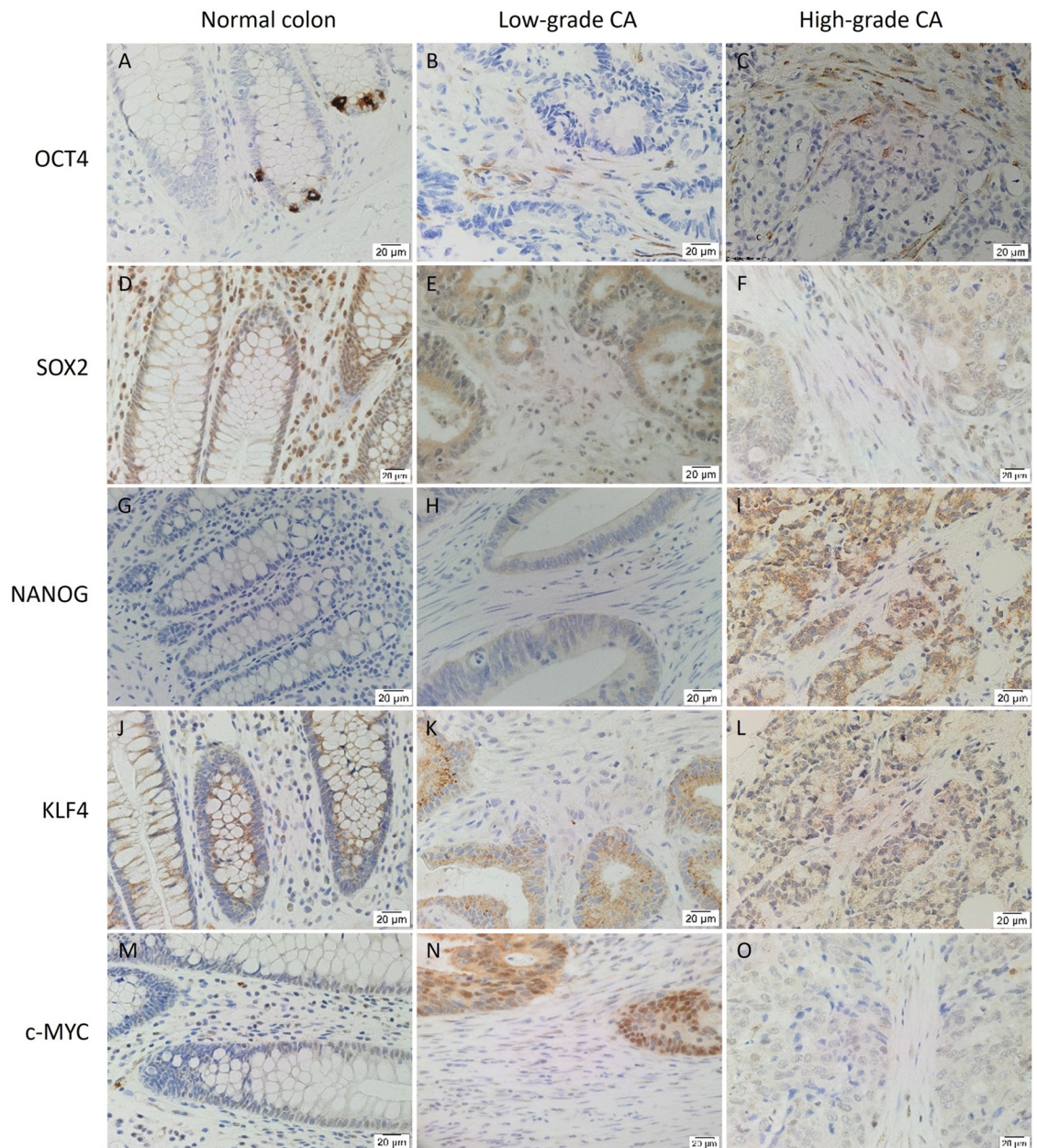


**Fig 1. DAB IHC staining.** Representative 3,3-diaminobenzidine immunohistochemical-stained images showing protein expression of induced-pluripotent stem cell markers OCT4 (A-C, brown), SOX2 (D-F, brown), NANOG (G-I, brown), KLF4 (J-L, brown) and c-MYC (M-O, brown) in normal colon (A,D,G,J,M), low-grade (B,F,H,K,N) and high-grade (C,F,I,L,O) colon adenocarcinoma tissue samples. Nuclei were counter-stained with hematoxylin (A-O, blue). Original magnification: 400x.

<https://doi.org/10.1371/journal.pone.0221963.g001>

epithelial cell cytoplasm (M). HGCA epithelium (N) exhibited more nuclear staining than LGCA (O) and NC (M) epithelium. KLF4 expression was seen in 22% of NC stromal cells of LGCA samples, and 44% of NC stromal cells of HGCA samples. Its expression was lower in LGCA than the NC samples with 14.4% of LGCA stromal cells staining positively, while 47.9% of stromal cells in HGCA samples expressed KLF4. Positive and negative controls are shown in S2 Fig, and cell counting data is displayed in S1 Table.

Two CSC subpopulations were identified by DAB IHC staining (Fig 2): one within the CA epithelium, with 9.7% of LGCA and 52.4% of HGCA epithelial cells expressing NANOG (Fig 2A); and the other within the CA stroma, with OCT4 being expressed by 24.3% of LGCA and 30.8% of HGCA stromal cells (Fig 2B). Discriminant value analysis revealed that all LGCA and HGCA tissue samples could be graded with 100% accuracy based on stromal expression of KLF4 in NC ( $p = 0.020$ ) and the tumors ( $p = 0.034$ ), and OCT4 ( $p = 0.001$ ) and NANOG ( $p = 0.026$ ) in CA epithelium (canonical correlation = 0.981; Wilkes Lambda = 0.037).

## IF IHC staining

IF IHC staining expanded on DAB IHC data by revealing localization of two iPSC markers simultaneously, as well as being a more sensitive detection method.

OCT4 (Fig 3A–3I, green) was expressed in the nucleus of few epithelial cells in NC (Fig 3A, 3D and 3G) and the cytoplasm of cells in the stroma of LGCA (Fig 3B, 3E and 3H) and HGCA (Fig 3C, 3F and 3I) tissue samples. KLF4 (Fig 3A–3C, red) stained positively in the cytoplasm of epithelial cells in NC (Fig 3A), LGCA (Fig 3B) and HGCA (Fig 3C), and some stromal cells in LGCA (Fig 3B, red) and HGCA (Fig 3C) samples. Epithelial cells in NC (Fig 3A) but not the stromal cells in LGCA (Fig 3B) or HGCA (Fig 3C) samples co-expressed OCT4 and KLF4 in their cytoplasm. NANOG (Fig 3D–3F and 3J–3L, red) was absent in NC (Fig 3D and 3J) but was seen in the cytoplasm of epithelial cells in LGCA (Fig 3E and 3K) and HGCA (Fig 3F and 3L) samples. SOX2 (Fig 3G–3I, red) was widely expressed in the epithelial cells and some stromal cells in both NC (Fig 3A), LGCA (Fig 3H) and HGCA (Fig 3I) tissue samples. SOX2 and OCT4 were co-expressed in epithelial cells in NC (Fig 3G) and stromal cells in LGCA (Fig 3H) and HGCA (Fig 3I). Cytoplasmic and nuclear staining of c-MYC (Fig 3J–3L, green) was weak in NC (Fig 3J), LGCA (Fig 3K) and HGCA (Fig 3L) epithelial and stromal cells. Stromal cells co-expressing OCT4 and SOX2 and those that stained positively for c-MYC had the same morphology and were assumed to be the same cell type. c-MYC and NANOG were co-expressed in HGCA epithelial cells (Fig 3L). From the above data we inferred that there was an epithelial subpopulation co-expressing NANOG, SOX2 and KLF4, and a stromal subpopulation co-expressing OCT4, SOX2 and c-MYC. Split images for Fig 3 are shown in S3 Fig.

## RT-qPCR

RT-qPCR demonstrated mRNA expression of all five iPSC markers in both the NC, LGCA and HGCA tissue samples (Fig 4). SOX2 mRNA was below the detection threshold in three NC tissue samples, and OCT4 was not detected in one NC tissue sample. NANOG, KLF4 and c-MYC mRNA was detected in all 12 NC tissue samples. All LGCA and HGCA tissue samples expressed mRNA for OCT4, NANOG, KLF4 and c-MYC. One LGCA and one HGCA tissue sample did not reach the detection threshold for SOX2.  $\Delta$ CT and fold-change data is displayed in S2 Table.

## ISH

ISH demonstrated the presence of mRNA for OCT4 (Fig 5A–5C, brown), SOX2 (Fig 5D–5F, brown), NANOG (Fig 5G–5I, brown), KLF4 (Fig 5J–5L, brown) and c-MYC (Fig 5M–5O, brown) in NC (Fig 5A, 5D, 5G, 5J and 5M), LGCA (Fig 5B, 5E, 5H, 5K and 5N) and HGCA (Fig 5C, 5F, 5I, 5L and 5O) tissue samples. Positive and negative controls are shown in S4 Fig, and cell counting data is displayed in S3 Table.

ISH cell counting demonstrated OCT4, SOX2, NANOG and c-MYC had higher mRNA levels in CA epithelium and stroma when compared to NC (Fig 6). Conversely, KLF4 was more

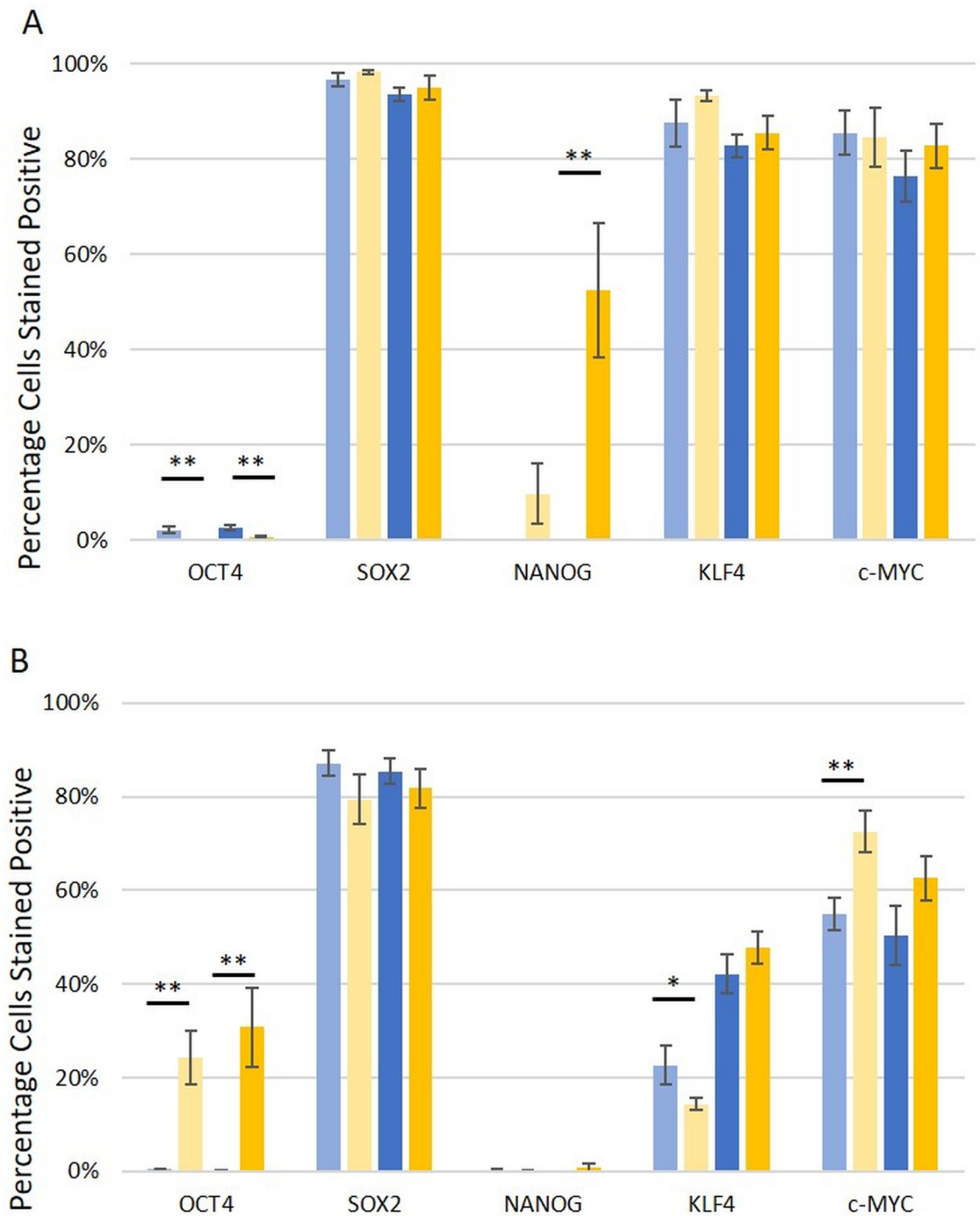


**Fig 2. DAB IHC data.** Percentage of cell population stained positively for induced-pluripotent stem cell markers OCT4, SOX2, NANOG, KLF4 and c-MYC by 3,3-diaminobenzidine immunohistochemical staining, for the epithelium (A) and the stroma (B). Normal colon samples from patients with low-grade colon adenocarcinoma (LGCA; pale blue, n = 9) are displayed separately to normal colon samples from patients with high-grade colon adenocarcinoma (HGCA; dark blue, n = 8). LGCA samples are shown in pale yellow (n = 10), and HGCA samples are shown in dark yellow (n = 8). Statistical significance with a p-value between 0.05 and 0.01 is shown by \*, and that for <0.01 is represented by \*\*. Error bars show standard error.

<https://doi.org/10.1371/journal.pone.0221963.g002>

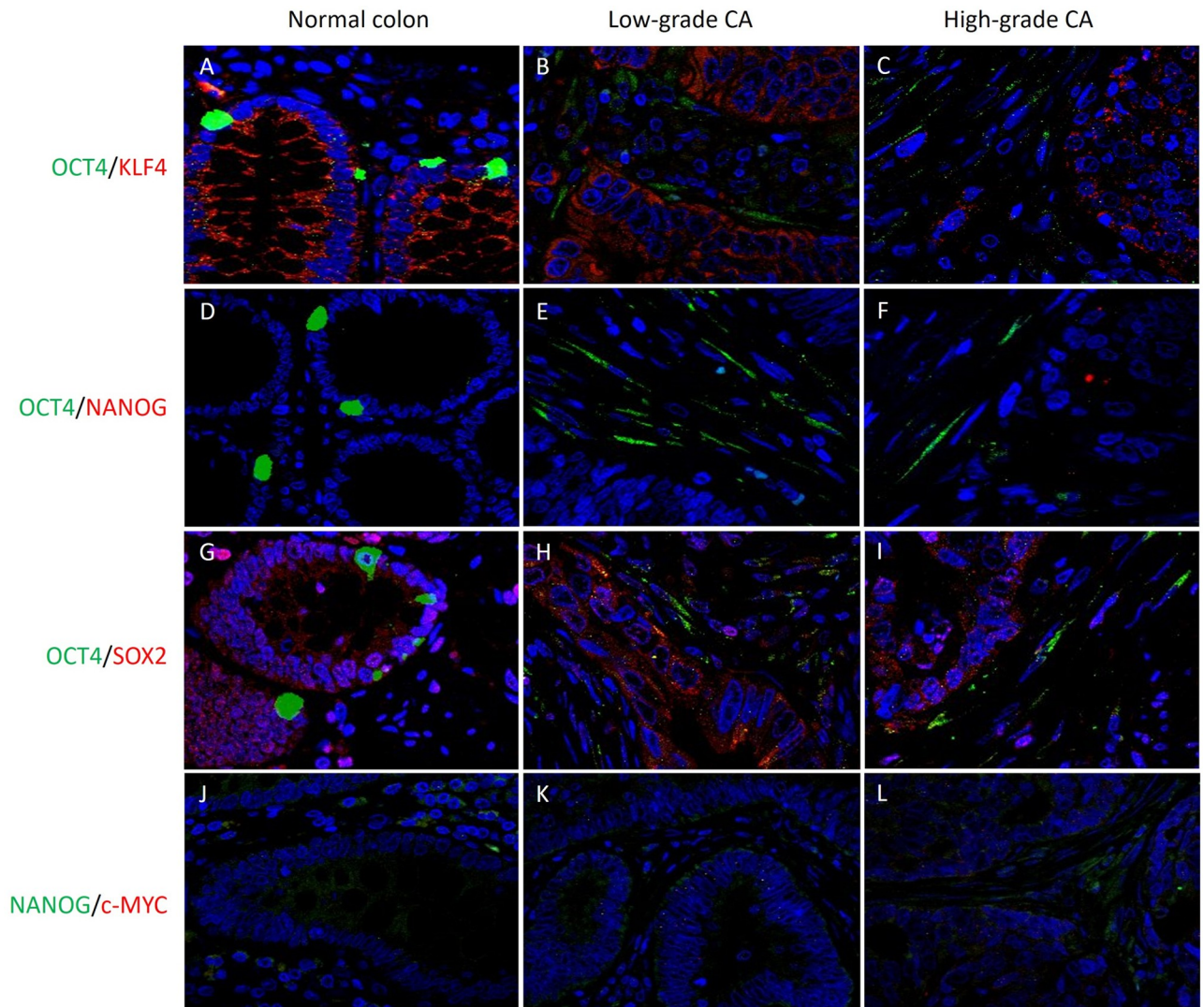


**Fig 3. IF IHC staining.** Representative immunofluorescence immunohistochemical-stained images showing protein expression of induced-pluripotent stem cell markers OCT4 (A–J, green), KLF4 (A–C, red), NANOG (D–G, H–J, red), SOX2 (H–J, red), and c-MYC (H–J, green) in normal colon (A,D,E,H), low-grade (B,E,F,I) and high-grade (C,F,G,J) colon adenocarcinoma tissue samples. Cell nuclei were counter-stained with 4', 6'-diamidino-2-phenylindole (A–L, blue). Original magnification: 400x.

<https://doi.org/10.1371/journal.pone.0221963.g003>

highly expressed in NC epithelium than that of CA. All differences between CA and their patient-matched NC tissue samples showed statistical significance ( $p < 0.05$ ).

## Discussion

This study investigated the transcriptional and translational expression of *OCT4*, *SOX2*, *NANOG*, *KLF4* and *c-MYC* to identify their presence in CSC subpopulations within CA.

RT-qPCR and ISH data for *SOX2* corroborated with each other, with RT-qPCR failing to detect *SOX2* in three NC samples and two CA samples, and ISH showing *SOX2* to be the least abundant in terms of the number of cells containing mRNA. However, *SOX2* was one of the most abundant markers at the protein level. Other studies have also shown an abundance of *SOX2* protein in both the nuclei and cytoplasm of CRC tumor cells [11, 19]. Furthermore, ISH



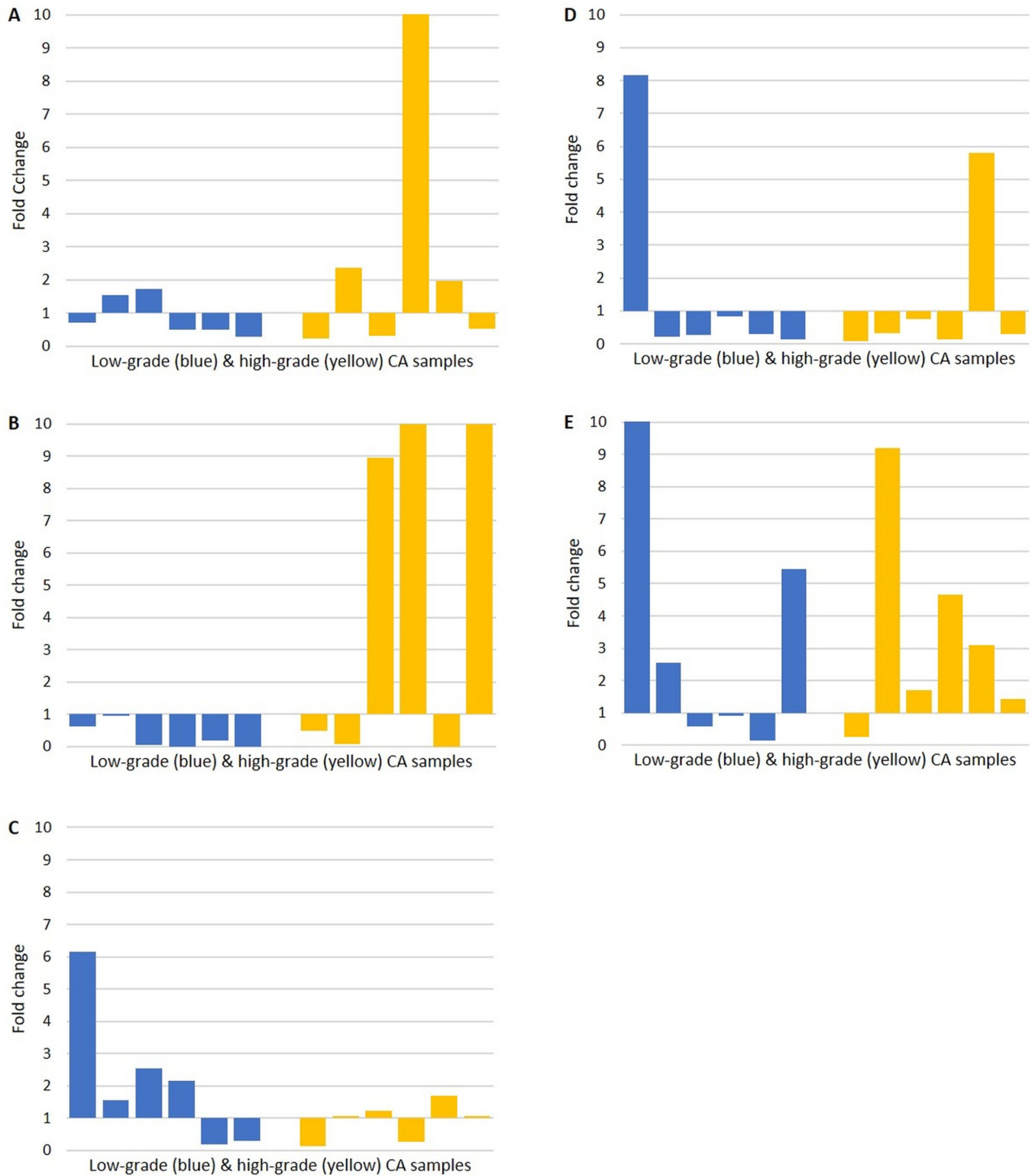


**Fig 4. RT-qPCR.** mRNA expression of induced-pluripotent stem cell markers *OCT4* (A), *SOX2* (B), *NANOG* (C), *KLF4* (D) and *c-MYC* (E) detected by RT-qPCR. Data displayed as the fold-change of gene expression in tumor samples relative to their patient-matched normal colon sample (Y-axis). A cohort of six LGCA tissue samples are shown in blue, and a cohort of six HGCA tissue samples are shown in yellow (X-axis).

<https://doi.org/10.1371/journal.pone.0221963.g004>

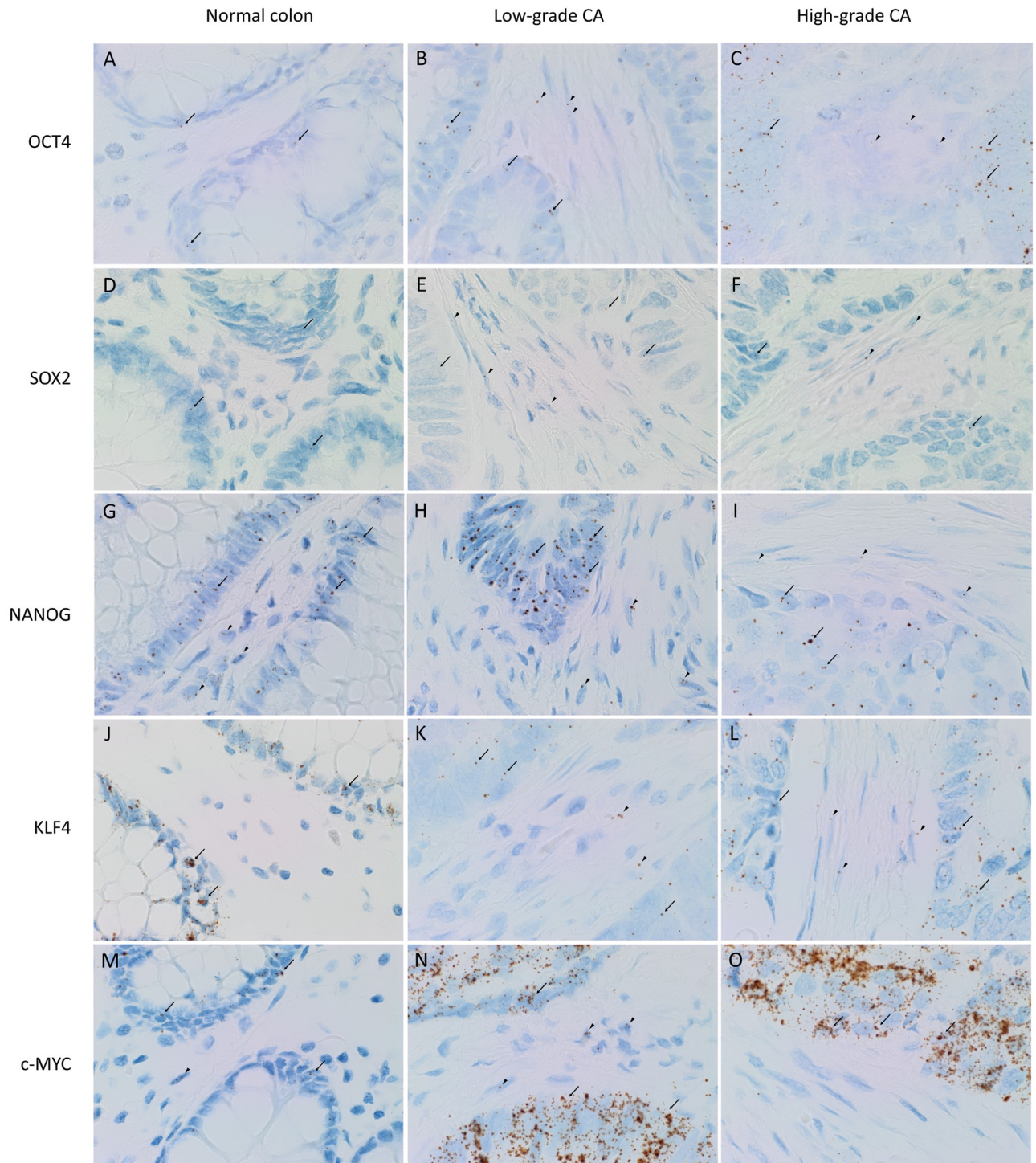


**Fig 5. In-situ hybridization.** Representative images of *in-situ* hybridization, showing mRNA expression of iPSC genes *OCT4* (A-C, brown), *SOX2* (D-F, brown), *NANOG* (G-I, brown), *KLF4* (J-L, brown) and *c-MYC* (M-O, brown) in the epithelial cells (arrows) and stromal cells (arrowheads) in normal colon (A,D,G,J,M), low-grade (B,E,H,K,N) and high-grade (C,F,I,L,O) colon adenocarcinoma tissue samples. Nuclei were counter-stained with hematoxylin (blue). Original magnification: 1000x.

<https://doi.org/10.1371/journal.pone.0221963.g005>

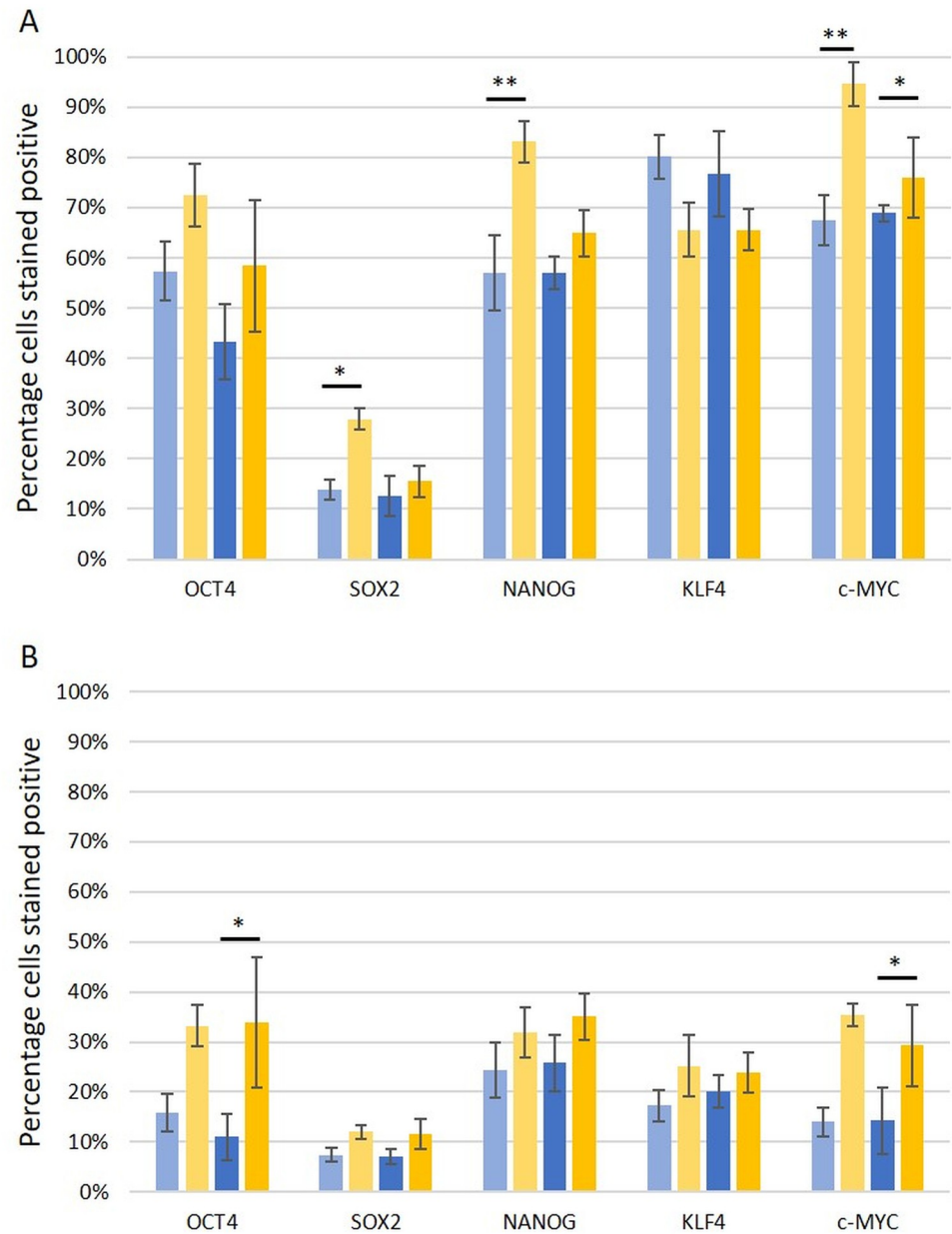


**Fig 6. In-situ hybridization data.** In-situ hybridization analysis showing the percentage of the cell population expressing mRNA for iPSC genes in the epithelium (A) and the stroma (B). Normal colon samples from patients with low-grade colon adenocarcinoma (LGCA) are represented in pale blue, normal colon samples from high-grade colon adenocarcinoma (HGCA) patients in dark blue, LGCA samples in pale yellow, and HGCA samples in dark yellow. Statistical significance with a *p*-value between 0.05 and 0.01 is shown by \*, and that for <0.01 is represented by \*\*. Error bars show standard error.

<https://doi.org/10.1371/journal.pone.0221963.g006>

showed abundance of *c-MYC* mRNA but DAB IHC staining showed weak protein staining, which may be due to the concentration of primary antibody used for DAB IHC staining.

*KLF4* has been previously studied in CRC and shown to be associated with epithelial-to-mesenchymal transition (EMT), cell migration and metastasis [16]. However, studies on the role of *KLF4* in cancer often yield conflicting results [31]. In NC, *KLF4* helps direct epithelial progenitor cells down the goblet cell lineage, the most abundant epithelial cell type in colonic

crypts [26]. As the grade of CA increases, the tumors are less differentiated, and this may explain the observation of decreased KLF4 in both LGCA and HGCA tumors, relative to NC. Our finding of higher KLF4 and OCT4 protein expression in the stroma of HGCA may reflect the migration of cancer cells by EMT, away from the epithelium, which has been postulated as a major factor in CRC progression [32]. Furthermore, when applying the concept of a stem cell hierarchy in cancer [6–8], we propose that cells at different levels of this hierarchy will express different combinations of these markers. For instance, OCT4 is known to be expressed by primitive stem cells such as ESCs [16, 33], whereas KLF4 is associated with a more differentiated phenotype [26, 27].

In this study, IF IHC staining identified two distinct CSC subpopulations: a NANOG<sup>+</sup>/OCT4<sup>-</sup> subpopulation localized to the epithelium, and an OCT4<sup>+</sup>/NANOG<sup>-</sup> subpopulation within the stroma. The stromal OCT4<sup>+</sup> subpopulation did not co-express NANOG or KLF4, but some stromal cells co-expressed OCT4 and SOX2. Similarly, in the epithelium, SOX2 and KLF4 staining was widespread but comparatively few of these cells were NANOG<sup>+</sup>. Based on the staining patterns, of these markers we infer the presence of two predominant CSC subpopulations in CA: an OCT4<sup>+</sup>/SOX2<sup>+</sup>/c-MYC<sup>+</sup> subpopulation within the stroma and a NANOG<sup>+</sup>/SOX2<sup>+</sup>/KLF4<sup>+</sup> subpopulation within the epithelium.

The literature correlating OCT4 and SOX2 expression with EMT and metastasis provides evidence supporting a stromal subpopulation expressing these markers that migrates away from the tumor [20, 31, 34]. Furthermore, NANOG is associated with maintenance of the stem-like phenotype of CSCs within the tumor, consistent with our observation of NANOG expression by some epithelial cells within the tumor [35]. KLF4 and c-MYC are associated with proliferation and differentiation and it is therefore not unexpected that these two markers were co-expressed by cells within CA [24, 27, 36].

Some stromal cells within CA that stained positively for OCT4 and c-MYC did not express KLF4 and SOX2. Some of these OCT4<sup>+</sup> stromal cells may be cancer-associated fibroblasts recruited by the tumor and induced to express OCT4 [37]. Alternatively, they may represent a CSC subpopulation that expresses stem cell markers other than the iPSC-related genes investigated in this study.

The patient-matched ‘normal colon’ samples used as a control may not represent true normal colon. Other limitations of this study include the lack of functional *in vitro* and *in vivo* investigations which will be the focus of future work.

The significance of OCT4, NANOG and KLF4 expression was seen in the discriminant values analysis. By considering the expression of stromal KLF4 and epithelial OCT4 and NANOG, all 18 CA cases could be accurately graded. This is demonstrated to be robust, with a canonical correlation of 0.981 representing a high degree of statistical significance, and a Wilks Lambda value of 0.037 showing that 96.3% of the variance between cases can be explained by these data.

Once validated, using the localization and expression levels of novel combinations of iPSC markers may provide a valuable tool to help guide patient management by further stratifying tumor grade, identifying cases with higher potential for metastasis or relapse, or tracking response to therapy.

## Supporting information

**S1 Fig. EpCAM DAB IHC staining.** Representative 3,3-diaminobenzidine immunohistochemical images showing protein expression of EPCAM (brown) in normal colon (A), low-grade colon adenocarcinoma (B&C), negative control (D), and high-grade colon adenocarcinoma (E&F). In all normal and tumor samples, EPCAM was expressed only by the epithelial

cells and not by stromal cells. Nuclei were counter-stained with hematoxylin (A-O, blue). Original magnification: 400x.  
(TIF)

**S2 Fig. DAB IHC controls.** Representative images of 3,3 diaminobenzidine immunohistochemical staining of human positive control tissues demonstrating the expected staining patterns on seminoma for OCT4 (A, brown) and NANOG (B, brown), skin for SOX2 (C, brown), normal breast tissue for KLF4 (D, brown) and prostatic tissue for c-MYC (E, brown). A section of colon adenocarcinoma probed with a matched anti-mouse isotype control and primary antibodies (F) confirmed the specificity of the secondary antibodies. Nuclei were counter-stained with hematoxylin (B-F, blue). Original magnification: 400X.  
(TIF)

**S3 Fig. IF IHC controls.** Individual stains of immunofluorescence immunohistochemical staining of normal colon (A,B,G,H,M,N,S,T), low-grade (C,D,I,J,O,P,U,V), and high-grade (E, F,K,L,Q,R,W,X) colon adenocarcinoma samples shown in Fig 3. Sections were co-stained for OCT4 (B,D,F,H,J,L,N,P,R, green) with KLF4 (A,C,E, red), NANOG (G,I,K, red) and SOX2 (M,O,Q, red); and c-MYC (T,V,X, green) with NANOG (S,U,W, red). Cell nuclei were counter-stained with 4'6-diamino-2-phenylindole (A-X). Scale bars: 20µm.  
(TIF)

**S4 Fig. ISH controls.** *In-situ* hybridization positive human control tissues for OCT4 (A, brown), NANOG (B, brown) and KLF4 (C, brown) on seminoma; SOX2 (D, brown) on normal skin, and c-MYC (E, brown) on normal colon. Negative control (F) performed on sections of colon adenocarcinoma tissue sample confirms specificity of secondary antibody. Original magnification: 1000x.  
(TIF)

**S1 Table. DAB IHC cell counting data.** Data showing the percentage of cells with any protein expression of each induced-pluripotent stem cell (iPSC) marker (weak, moderate or strong) by cells in the epithelium and those in the stoma with the standard error values in brackets. LGCA, low-grade colon adenocarcinoma tissue samples; HGCA, high-grade colon adenocarcinoma tissue samples. NCLG, normal colon tissue from patients with LGCA; NCHG, normal colon tissue from patients with HGCA. Significance values for comparisons between LGCA and HGCA tissue samples and their patient-matched normal colon tissues, for cells in the epithelium and those in the stoma: a p-value between 0.05 and 0.01 is shown by \*, and <0.01 represented by \*\*.  
(PDF)

**S2 Table. RT-qPCR data.** RT-qPCR data showing expression of induced-pluripotent stem cell (iPSC) markers *OCT4*, *SOX2*, *NANOG*, *KLF4* and *c-MYC*.  $\Delta$ CT values calculated by comparing the gene of interest to housekeeper *GAPDH*, and  $\Delta\Delta$ CT values by comparing high-grade (HG) and low-grade (LG) tumors to their patient-matched normal colon samples.  $\Delta\Delta$ CT values used to calculate fold changes using the equation  $2^{(-\Delta\Delta CT)}$ .  
(PDF)

**S3 Table. ISH cell counting data.** Data showing the percentage of cells with mRNA expression of each induced-pluripotent stem cell (iPSC) marker in the epithelium and in the stoma, with the standard error values in brackets. LGCA, low-grade colon adenocarcinoma tissue samples; HGCA, high-grade colon adenocarcinoma tissue samples. NCLG, normal colon tissue from patients with LGCA; NCHG, normal colon tissue from patients with HGCA. Significance values for comparisons between LGCA and HGCA tissue samples and their patient-matched

normal colon tissues, for cells in the epithelium and those in the stroma: a p-value between 0.05 and 0.01 is shown by \*, and <0.01 represented by \*\*.  
(PDF)

**S1 Datasets. Raw data.** Raw data collected and analyzed during this study is provided, including anonymous patient data, DAB IHC cell counting data, discriminant function analysis output, *in-situ* hybridization cell counting data, raw RT-qPCR CT values, and cell counting statistics.  
(ZIP)

## Acknowledgments

We thank Ms Liz Jones and Dr Helen Brasch of the Gillies McIndoe Research Institute for their assistance in IHC and ISH staining; and assessment of the tissue samples and interpretation of the DAB IHC staining, respectively. We are grateful to Dr John Groom from Wakefield Hospital and he and his colleagues' Drs Atul Dhabuwala, Stephen Purchas and James Teitjens at the Department of General Surgery at Hutt Hospital, for providing tissue samples that were recruited to the Gillies McIndoe Research Institute Tissue Bank.

## Author Contributions

**Conceptualization:** Matthew J. Munro, Susrutha K. Wickremesekera, Lifeng Peng, Tinte Itinteang, Swee T. Tan.

**Data curation:** Matthew J. Munro.

**Formal analysis:** Matthew J. Munro, Lifeng Peng, Reginald W. Marsh, Swee T. Tan.

**Funding acquisition:** Swee T. Tan.

**Investigation:** Matthew J. Munro.

**Methodology:** Matthew J. Munro.

**Project administration:** Tinte Itinteang, Swee T. Tan.

**Resources:** Swee T. Tan.

**Supervision:** Susrutha K. Wickremesekera, Lifeng Peng, Tinte Itinteang, Swee T. Tan.

**Validation:** Matthew J. Munro, Lifeng Peng, Reginald W. Marsh, Tinte Itinteang, Swee T. Tan.

**Visualization:** Matthew J. Munro.

**Writing – original draft:** Matthew J. Munro, Susrutha K. Wickremesekera, Lifeng Peng, Tinte Itinteang, Swee T. Tan.

**Writing – review & editing:** Matthew J. Munro, Susrutha K. Wickremesekera, Lifeng Peng, Reginald W. Marsh, Tinte Itinteang, Swee T. Tan.

## References

1. Khalek FJA, Gallicano GI, Mishra L. Colon Cancer Stem Cells. *Gastrointestinal Cancer Research: GCR*. 2010;(Suppl 1):S16–S23. PMID: [21472043](https://pubmed.ncbi.nlm.nih.gov/21472043/)
2. Kreso A, Dick JE. Evolution of the cancer stem cell model. *Cell Stem Cell*. 2014; 14(3):275–91. <https://doi.org/10.1016/j.stem.2014.02.006> PMID: [24607403](https://pubmed.ncbi.nlm.nih.gov/24607403/).
3. Zheng S, Xin L, Liang A, Fu Y. Cancer stem cell hypothesis: a brief summary and two proposals. *Cyto-technology*. 2013; 65(4):505–12. <https://doi.org/10.1007/s10616-012-9517-3> PMID: [23250634](https://pubmed.ncbi.nlm.nih.gov/23250634/)

4. Shimokawa M, Ohta Y, Nishikori S, Matano M, Takano A, Fujii M, et al. Visualization and targeting of LGR5+ human colon cancer stem cells. *Nature*. 2017; 545(7653):187–92. <https://doi.org/10.1038/nature22081> PMID: 28355176.
5. Tang DG. Understanding cancer stem cell heterogeneity and plasticity. *Cell Res*. 2012; 22(3):457–72. <https://doi.org/10.1038/cr.2012.13> PMID: 22357481
6. Seaberg RM, van der Kooy D. Stem and progenitor cells: the premature desertion of rigorous definitions. *Trends Neurosci*. 2003; 26(3):125–31. Epub 2003/02/20. [https://doi.org/10.1016/S0166-2236\(03\)00031-6](https://doi.org/10.1016/S0166-2236(03)00031-6) PMID: 12591214.
7. Gage FH. Mammalian neural stem cells. *Science*. 2000; 287(5457):1433–8. Epub 2000/02/26. <https://doi.org/10.1126/science.287.5457.1433> PMID: 10688783.
8. Bradshaw A, Wickremsekera A, Tan ST, Peng L, Davis PF, Itinteang T. Cancer Stem Cell Hierarchy in Glioblastoma Multiforme. *Frontiers in Surgery*. 2016; 3(21). <https://doi.org/10.3389/fsurg.2016.00021> PMID: 27148537
9. Takahashi K, Yamanaka S. Induction of pluripotent stem cells from mouse embryonic and adult fibroblast cultures by defined factors. *Cell*. 2006; 126(4):663–76. <https://doi.org/10.1016/j.cell.2006.07.024> PMID: 16904174.
10. Yu J, Vodyanik MA, Smuga-Otto K, Antosiewicz-Bourget J, Frane JL, Tian S, et al. Induced pluripotent stem cell lines derived from human somatic cells. *Science*. 2007; 318(5858):1917–20. <https://doi.org/10.1126/science.1151526> PMID: 18029452.
11. Amini S, Fathi F, Mobalegi J, Sofimajidpour H, Ghadimi T. The expressions of stem cell markers: Oct4, Nanog, Sox2, nucleostemin, Bmi, Zfx, Tcf1, Tbx3, Dppa4, and Esrrb in bladder, colon, and prostate cancer, and certain cancer cell lines. *Anat Cell Biol*. 2014; 47(1):1–11. <https://doi.org/10.5115/acb.2014.47.1.1> PMID: 24693477
12. Hu J, Li J, Yue X, Wang J, Liu J, Sun L, et al. Expression of the cancer stem cell markers ABCG2 and OCT-4 in right-sided colon cancer predicts recurrence and poor outcomes. *Oncotarget*. 2017; 8(17):28463–70. <https://doi.org/10.18632/oncotarget.15307> PMID: 28212529
13. Wen K, Fu Z, Wu X, Feng J, Chen W, Qian J. Oct-4 is required for an antiapoptotic behavior of chemoresistant colorectal cancer cells enriched for cancer stem cells: effects associated with STAT3/Survivin. *Cancer Lett*. 2013; 333(1):56–65. <https://doi.org/10.1016/j.canlet.2013.01.009> PMID: 23340171.
14. Gazouli M, Roubelakis MG, Theodoropoulos GE, Papailiou J, Vaiopoulou A, Pappa KI, et al. OCT4 spliced variant OCT4B1 is expressed in human colorectal cancer. *Mol Carcinog*. 2012; 51(2):165–73. Epub 2011/04/12. <https://doi.org/10.1002/mc.20773> PMID: 21480394.
15. Zhang S, Cui W. Sox2, a key factor in the regulation of pluripotency and neural differentiation. *World J Stem Cells*. 2014; 6(3):305–11. <https://doi.org/10.4252/wjsc.v6.i3.305> PMID: 25126380
16. Hadjimichael C, Chanoumidou K, Papadopoulou N, Arampatzis P, Papamatheakis J, Kretsovali A. Common stemness regulators of embryonic and cancer stem cells. *World J Stem Cells*. 2015; 7(9):1150–84. <https://doi.org/10.4252/wjsc.v7.i9.1150> PMID: 26516408
17. Avery S, Inniss K, Moore H. The regulation of self-renewal in human embryonic stem cells. *Stem Cells Dev*. 2006; 15(5):729–40. <https://doi.org/10.1089/scd.2006.15.729> PMID: 17105408.
18. Masui S, Nakatake Y, Toyooka Y, Shimosato D, Yagi R, Takahashi K, et al. Pluripotency governed by Sox2 via regulation of Oct3/4 expression in mouse embryonic stem cells. *Nat Cell Biol*. 2007; 9(6):625–35. <https://doi.org/10.1038/ncb1589> PMID: 17515932.
19. Talebi A, Kianersi K, Beiraghdar M. Comparison of gene expression of SOX2 and OCT4 in normal tissue, polyps, and colon adenocarcinoma using immunohistochemical staining. *Adv Biomed Res*. 2015; 4:234. <https://doi.org/10.4103/2277-9175.167958> PMID: 26645019
20. Neumann J, Bahr F, Horst D, Kriegl L, Engel J, Luque RM, et al. SOX2 expression correlates with lymph-node metastases and distant spread in right-sided colon cancer. *BMC Cancer*. 2011; 11:518. <https://doi.org/10.1186/1471-2407-11-518> PMID: 22168803
21. Pan G, Thomson JA. Nanog and transcriptional networks in embryonic stem cell pluripotency. *Cell Res*. 2007; 17(1):42–9. <https://doi.org/10.1038/sj.cr.7310125> PMID: 17211451.
22. Ibrahim EE, Babaei-Jadidi R, Saadeddin A, Spencer-Dene B, Hossaini S, Abuzinadah M, et al. Embryonic NANOG activity defines colorectal cancer stem cells and modulates through AP1- and TCF-dependent mechanisms. *Stem Cells*. 2012; 30(10):2076–87. <https://doi.org/10.1002/stem.1182> PMID: 22851508.
23. Lee KS, Kwak Y, Nam KH, Kim DW, Kang SB, Choe G, et al. c-MYC Copy-Number Gain Is an Independent Prognostic Factor in Patients with Colorectal Cancer. *PLoS One*. 2015; 10(10):e0139727. Epub 2015/10/02. <https://doi.org/10.1371/journal.pone.0139727> PMID: 26426996
24. Martini M, Basso M, Coccomazzi A, Cenci T, Strippoli A, Fiorentino V, et al. c-Myc expression as a key-marker in the colorectal cancer resistance to EGFR inhibitors. *Journal of Clinical Oncology*. 2016; 34(15\_suppl):e15034–e. [https://doi.org/10.1200/JCO.2016.34.15\\_suppl.e15034](https://doi.org/10.1200/JCO.2016.34.15_suppl.e15034)

25. Leng Z, Tao K, Xia Q, Tan J, Yue Z, Chen J, et al. Kruppel-like factor 4 acts as an oncogene in colon cancer stem cell-enriched spheroid cells. *PLoS One*. 2013; 8(2):e56082. <https://doi.org/10.1371/journal.pone.0056082> PMID: 23418515
26. May CL, Kaestner KH. Gut endocrine cell development. *Mol Cell Endocrinol*. 2010; 323(1):70–5. <https://doi.org/10.1016/j.mce.2009.12.009> PMID: 20025933
27. Hu R, Zuo Y, Zuo L, Liu C, Zhang S, Wu Q, et al. KLF4 Expression Correlates with the Degree of Differentiation in Colorectal Cancer. *Gut Liver*. 2011; 5(2):154–9. Epub 2011/08/05. <https://doi.org/10.5009/gnl.2011.5.2.154> PMID: 21814594
28. Fleming M, Ravula S, Tatishchev SF, Wang HL. Colorectal carcinoma: Pathologic aspects. *J Gastrointest Oncol*. 2012; 3(3):153–73. <https://doi.org/10.3978/j.issn.2078-6891.2012.030> PMID: 22943008
29. Humphries HN, Wickremesekera SK, Marsh RW, Brasch HD, Mehrotra S, Tan ST, et al. Characterization of Cancer Stem Cells in Colon Adenocarcinoma Metastasis to the Liver. *Front Surg*. 2017; 4:76. Epub 2018/02/07. <https://doi.org/10.3389/fsurg.2017.00076> PMID: 29404335
30. Ram R, Brasch HD, Dunne JC, Davis PF, Tan ST, Itinteang T. The Identification of Three Cancer Stem Cell Subpopulations within Moderately Differentiated Lip Squamous Cell Carcinoma. *Front Surg*. 2017; 4:12. Epub 2017/03/23. <https://doi.org/10.3389/fsurg.2017.00012> PMID: 28321397
31. Muller M, Hermann PC, Liebau S, Weidgang C, Seufferlein T, Kleger A, et al. The role of pluripotency factors to drive stemness in gastrointestinal cancer. *Stem Cell Res*. 2016; 16(2):349–57. Epub 2016/02/22. <https://doi.org/10.1016/j.scr.2016.02.005> PMID: 26896855.
32. Loboda A, Nebozhyn MV, Watters JW, Buser CA, Shaw PM, Huang PS, et al. EMT is the dominant program in human colon cancer. *BMC Med Genomics*. 2011; 4:9. Epub 2011/01/22. <https://doi.org/10.1186/1755-8794-4-9> PMID: 21251323
33. Shi G, Jin Y. Role of Oct4 in maintaining and regaining stem cell pluripotency. *Stem Cell Res Ther*. 2010; 1(5):39. <https://doi.org/10.1186/scrt39> PMID: 21156086
34. Dai X, Ge J, Wang X, Qian X, Zhang C, Li X. OCT4 regulates epithelial-mesenchymal transition and its knockdown inhibits colorectal cancer cell migration and invasion. *Oncol Rep*. 2013; 29(1):155–60. <https://doi.org/10.3892/or.2012.2086> PMID: 23076549.
35. Zhang J, Espinoza LA, Kinders RJ, Lawrence SM, Pfister TD, Zhou M, et al. NANOG Modulates Stemness in Human Colorectal Cancer. *Oncogene*. 2013; 32(37):4397–405. <https://doi.org/10.1038/onc.2012.461> PMID: 23085761
36. Halim S, Markert EK, Vazquez A. Analysis of cell proliferation and tissue remodelling uncovers a KLF4 activity score associated with poor prognosis in colorectal cancer. *Br J Cancer*. 2018; 119(7):855–63. Epub 2018/10/06. <https://doi.org/10.1038/s41416-018-0253-0> PMID: 30287917.
37. Som A, Bloch S, Ippolito JE, Achilefu S. Acidic extracellular pH of tumors induces octamer-binding transcription factor 4 expression in murine fibroblasts in vitro and in vivo. *Sci Rep*. 2016; 6:27803. Epub 2016/06/16. <https://doi.org/10.1038/srep27803> PMID: 27302093